Effects of hydroxyl group distribution on the reactivity, stability and optical properties of fullerenols

2008 Nanotechnology 19 365703

(http://iopscience.iop.org/0957-4484/19/36/365703)

Nanotechnology **19** (2008) 365703 (7pp) doi:10.1088/0957-4484/19/36/365703

Effects of hydroxyl group distribution on the reactivity, stability and optical properties of fullerenols

Eudes E Fileti[1], Roberto Rivelino[2], F de Brito Mota[2] and Thaciana Malaspina[3]

[1] Centro de Ciências Naturais e Humanas, Universidade Federal do ABC, 09210-270 Santo André, SP, Brazil
[2] Instituto de Física, Universidade Federal da Bahia, 40210-340 Salvador, BA, Brazil
[3] Instituto de Química, Universidade de São Paulo, 05513-970 São Paulo, SP, Brazil

E-mail: fileti@ufabc.edu.br, rivelino@ufba.br and fbmota@ufba.br

Received 17 April 2008, in final form 20 June 2008
Published 28 July 2008
Online at stacks.iop.org/Nano/19/365703

Abstract

We investigate the impact of hydroxyl groups on the properties of $C_{60}(OH)_n$ systems, with $n = 1, 2, 3, 4, 8, 10, 16, 18, 24, 32$ and 36 by means of first-principles density functional theory calculations. A detailed analysis from the local density of states has shown that adsorbed OH groups can induce dangling bonds in specific carbon atoms around the adsorption site. This increases the tendency to form polyhydroxylated fullerenes (fullerenols). The structural stability is analyzed in terms of the calculated formation enthalpy of each species. Also, a careful examination of the electron density of states for different fullerenols shows the possibility of synthesizing single molecules with tunable optical properties.

S Supplementary data are available from stacks.iop.org/Nano/19/365703

(Some figures in this article are in colour only in the electronic version)

1. Introduction

The unusual properties of fullerenes continue to be an issue of considerable interest, despite their continuous experimental and theoretical studies since the mass spectroscopic detection of C_{60} in 1985 [1]. Nowadays, water-soluble fullerenes have been considered as promising materials in different areas [2–4]. These systems are particularly exciting in the context of chemical functionalization [5], which is rapidly increasing towards biological and materials applications [6–11]. Recently, a great deal of biological activity of hydroxylated C_{60} or $C_{60}(OH)_n$, so-called fullerenols, has been reported [12–16]. Usually, these molecules exhibit different cytotoxic actions in cell lines [17–21] depending on the number of hydroxyl groups attached to the fullerene cage. In a diverse fashion, the optical properties of molecular films based on fullerenols have been investigated aiming at efficient polymer–fullerene solar cells [22]. Also, the possibility of having highly hydroxylated fullerene cages is directly related to the design of new materials with tunable optical properties [23–25].

The chemical modification of fullerenes by incorporating OH groups on their carbon surface yields a variety of polyhydroxylated structures [$C_{60}(OH)_n$] exhibiting different degrees of solubility and antioxidant activities in the aqueous environment [18, 19, 26–28]. These characteristic features clearly reveal the complexity of both the geometric and electronic structures of fullerenols [29–31]. Thus, their electronic properties and reactivity will strongly depend on the OH number, as well as its precise position on the carbon cage. Despite having relatively simple chemical routes to synthesize fullerenols [32, 33], analytical techniques capable of determining the exact hydroxyl disposition onto the fullerene surface is still lacking. It is thus worthwhile to provide additional information about the precise structure beyond the experimental evidence. In this sense, appropriate first-principles calculations emerge as a reliable method to efficiently identify the structure of these polyhydroxylated C_{60} derivatives based on their electronic properties analysis.

Another important aspect concerning fullerenols is related to their high reactivity in the aqueous environment. As recently

shown by Pickering and Wiesner [28], these molecules can work as efficient photosensitizers of reactive oxygen (e.g. singlet oxygen and superoxide) under ultraviolet irradiation. Conversely, highly hydroxylated C_{60} may also behave as free radical scavengers or antioxidant agents [17–19], reducing the reactive oxygen species formation. Indeed, the mechanisms behind the reactivity of $C_{60}(OH)_n$ are still rather incomplete from the electronic structure viewpoint. Therefore, high level theoretical investigations on the structural and electronic properties are highly desirable. This is the aim of this paper. First, we employ first-principles density functional theory (DFT) methods to obtain fully relaxed minimum energy structures of fullerenols with various degrees of hydroxylation. Second, we examine their electronic properties as a function of coverage and spatial distribution of hydroxyl groups. Finally, the reactivity and tunable optical properties are investigated from the electronic states of the fullerenols.

2. Methods and calculations

The specific behavior of fullerenols is determined by their structural flexibility, which is due to the rotation of the OH groups around the axes going through the C–O bond and the distribution of these groups onto different carbon sites of the fullerene surface. For this reason, the determination of the global minima represents a rather difficult task. More exactly, very efficient searching procedures would be required to scan the whole potential energy surfaces (PES). Of course, the localization of all stationary points on the PES is beyond the capability of *ab initio* geometry optimizations. Thus, we select representative low energy configurations of $C_{60}(OH)_n$, with $n = 1, 2, 3, 4, 8, 10, 16, 18, 24, 32$ and 36. These are obtained by performing DFT calculations within the gradient-corrected approximation (GGA) with the BLYP proposal [34, 35], as implemented in the SIESTA program [36]. The nonlocal norm-conserving scalar Troullier–Martins pseudopotential has been used and the Kohn–Sham (KS) eigenstates are expanded using a linear combination of numerical atomic orbitals (NAO), representing a basis set with double-ζ quality and polarization function (DZP) [37]. An equivalent plane-wave cutoff radius of 200 Ry for the grid integration is utilized. Structural optimizations are performed until the residual force on each atom becomes smaller than 0.01 eV $Å^{-1}$. Only the Γ-point in the Brillouin zone has been sampled in these calculations.

In order to obtain good estimates for the enthalpy of formation, we re-optimize the fullerenol structures within the all-electron scheme using the hybrid GGA B3LYP functional [38, 39] combined with the 6–31G(d,p) basis set. This level of theory is performed employing the GAUSSIAN 03 program [40]. The vibrational frequencies are calculated within the harmonic approximation, from which we obtain the zero-point vibration energy corrections. Thus, we have calculated the enthalpy of formation (ΔH_F) for the different structures as follows:

$$\Delta H_F = E_{C_{60}(OH)_n} - E_{C_{60}} - nE_{OH}, \quad (1)$$

where $E_{C_{60}(OH)_n}$ is the total energy of the hydroxylated fullerene, $E_{C_{60}}$ is the total energy of the bare fullerene and E_{OH} is the total energy of an isolated hydroxyl, all of them including contributions from translational, rotational and vibrational motions, and thermal correction at 298 K and 1 atm.

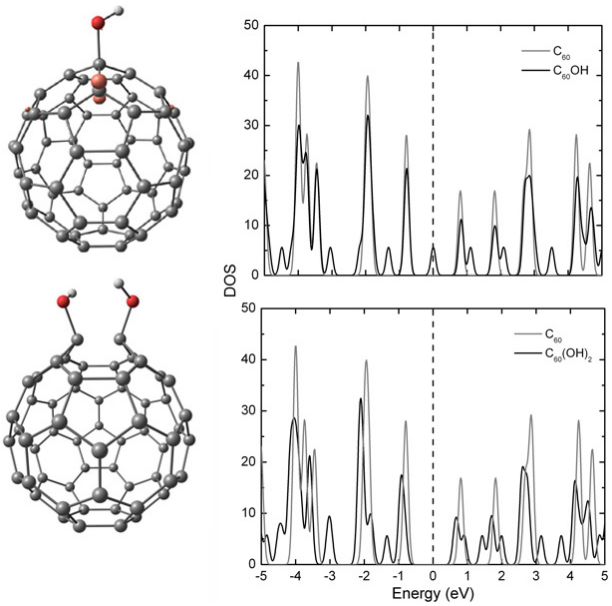

Figure 1. Charge density plot of $C_{60}OH$ from the local density of states (LDOS) calculated with BLYP/DZP for the electronic states around the Fermi level (top left side); and its corresponding total density of states (DOS) compared with that of the isolated C_{60} molecule (top right side). In the bottom a similar analysis is performed for the $C_{60}(OH)_2$ system. In this case the π-bond reconstruction on the carbon cage surface following the second OH adsorption removes electron states from the gap.

3. Results and discussion

The optimized structures of our hydroxylated fullerene systems are shown here and in the supplementary data (figure S1 available at stacks.iop.org/Nano/19/365703). Here, in figure 1 (top) we show a general aspect related to fullerenes containing an odd number of hydroxyl groups (i.e. electron open-shell fullerenols). For example, analyzing the KS electron states from the density of states (DOS) of the electron open-shell $C_{60}OH$ system, we notice a dangling bond in the nearest-neighbor carbon atom belonging to a pentagon ring (left top side). This is supported by the corresponding DOS plotted in figure 1 (top), where a localized electron state of p character appears in the Fermi energy level (vertical dashed lines). In fact, the OH adsorption induces a notable redistribution of charge on the C_{60} cage, increasing its chemical reactivity. The carbon atom directly involved in the binding process loses electron density to the OH group, as well as to the carbon atoms around the adsorption site. It is also possible to observe a similar pattern in $C_{60}(OH)_3$ (see figure S2 in the supplementary data (available at stacks.iop.org/Nano/19/365703)). Actually, when we saturate $C_{60}OH$ by incorporating a second OH group the localized state is removed from the gap. This can be clearly realized in the DOS displayed in figure 1 (bottom). Interestingly, the removal of electron states from the Fermi level does not depend on the location of the second OH group

on the carbon cage. This is mainly attributed to the π-bond reconstruction by electron delocalization following the adsorption of a second hydroxyl group.

As expected for exohedral fullerene-doped compounds, we have obtained that an adsorbed OH group on the fullerene surface causes an appreciable perturbation in the geometry of the fullerene cage. The lengths of the nearest-neighbor C–C bonds to the OH-adsorbed site are increased by approximately 0.1 Å compared to the ones around nonadsorbed carbon atoms. At the BLYP/DZP level, the relaxed C–O and O–H bond lengths are, respectively, 1.469 and 0.992 Å, along with a C–O–H angle of 106.8° in the $C_{60}OH$ molecule. By re-optimizing the geometry with the all-electron B3LYP/6–31G(d,p) method, the C–O and O–H bond distances decrease, respectively, to 1.431 and 0.969 Å, while the C–O–H angle gives a very near value of 107.4°. The addition of a second hydroxyl directly on the carbon containing the dangling bond leads to an OH-antisymmetric $C_{60}(OH)_2$ configuration (figure 1, bottom), with an O···O bond distance of 2.542 Å, by using B3LYP/6–31G(d,p). Now, the C–O and O–H bond lengths and the C–O–H angle are, respectively, 1.427, 0.970 Å and 106.5°. The C–C bond length between the two OH-adsorbed sites is 1.623 Å, which is 0.2 Å larger than the nonadsorbed equivalent bonds, exhibiting pentagonal vertices tilted away from the surface with dihedral angles around 12°.

The present theoretical findings suggest that the electronic properties of fullerenols can be tuned by tailoring both the OH number and disposition on the fullerene surface. Therefore, it is even interesting to analyze these properties by considering higher hydroxylated fullerenes (figure 2). For instance, by increasing the fullerene coverage to 8 OH groups we can observe, from the DOS (figures 3(a) and (b)), electronic states with essentially carbon p character in the HOMO–LUMO energy gap, which are strongly dependent on the disposition of the hydroxyl groups on the fullerene surface. As can be seen, the energy gap obtained for the more symmetrical $C_{60}(OH)_8$ structure (figure 2(a)) is a little reduced in comparison to pristine C_{60}, whereas for the less symmetrical $C_{60}(OH)_8$ structure (figure 2(b)) the bandgap is considerably reduced because of the additional states around the Fermi level (figure 3(b)). Partial charge densities associated with these states are shown in figure 4 (left). In the case of $C_{60}(OH)_8$, both HOMO and LUMO states consist of much more degenerate p states in the symmetrical structure than in the less symmetrical one. It becomes clear from this point that the precise position of the OH groups plays an important role to control the electronic states in the gap of these complexes.

Also, this feature can be reinforced by considering the two structural isomers of $C_{60}(OH)_{10}$ given in figures 2(c) and (d). In the first one, the corresponding bandgap shown in figure 3(c) remains almost unchanged (in comparison to the one of C_{60}), with both the valence and conduction bands slightly shifted to higher energies. Their corresponding partial charge densities of the HOMO and LUMO states are shown in figure 4 (right). For the isomer shown in figure 2(c), it is still noticed there are endohedral π-bonds in the HOMO states. On the other hand, the open-cage structure (figure 2(d)) presents only states of carbon p character in the gap, as shown in figure 4 (right). These electron densities are in agreement with the DOS exhibited in figures 3(c) and (d). The right attribution of these states is shown in detail in our calculated projected-DOS given in figure S2 (PDOS given in the supplementary data (available at stacks.iop.org/Nano/19/365703)). Up to this point these results have already revealed interesting aspects concerning the structural and electronic properties of some moderately hydroxylated fullerenes. Going to higher hydroxylated systems, such as $C_{60}(OH)_{16}$ and $C_{60}(OH)_{18}$, shown in figures 2(e) and (f), respectively, and $C_{60}(OH)_{24}$ (figure S3 in the supplementary data available at stacks.iop.org/Nano/19/365703), we also observe similar tunable electronic properties. These are clearly dependent on the distribution of adsorbed OH groups on the surface. Besides, the specific location of each hydroxyl group will have an important effect on the stability of all these species.

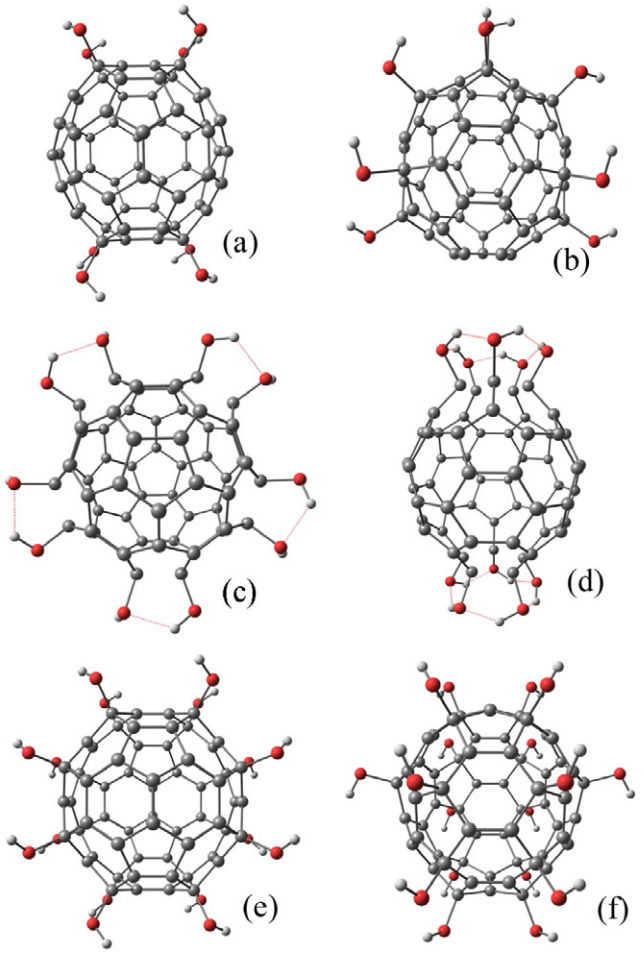

Figure 2. Optimized structures for different $C_{60}(OH)_n$ molecules: $n = 8$ (a) and (b), $n = 10$ (c) and (d), $n = 16$ (e) and $n = 18$ (f). The optimizations are carried out using the GGA BLYP/DZP level for residual force on each atom smaller than 0.01 eV $Å^{-1}$.

The calculated enthalpy of formation (equation (1)) of a series of fullerenols as a function of the OH number is shown in figure 5. Only the lower energy isomers are considered in this graph. For instance, the isomers with 8 and 10 hydroxyl groups correspond to structures (a) and (c), respectively, already presented in figure 2. Evidently, this is a small sample of many

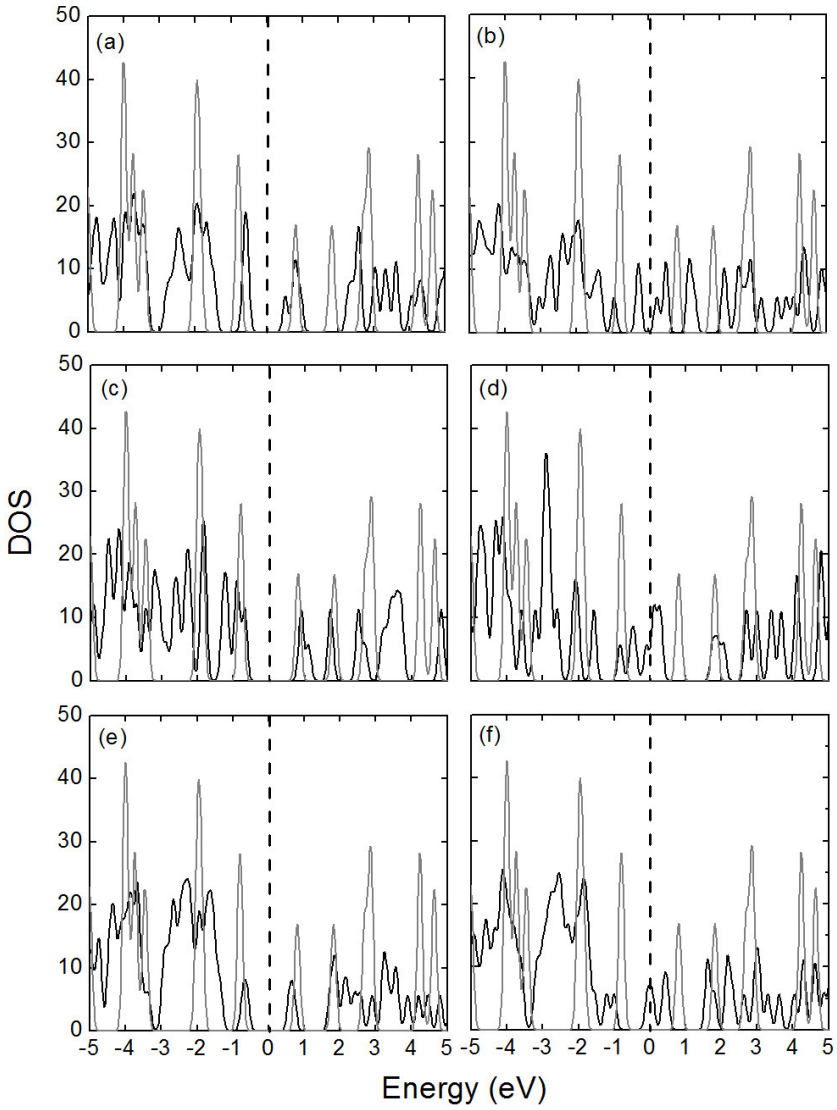

Figure 3. Total density of states (DOS) calculated at the BLYP/DZP level for the fullerenols displayed in figure 2. $C_{60}(OH)_8$ isomers (a) and (b), $C_{60}(OH)_{10}$ isomers (c) and (d), $C_{60}(OH)_{16}$ (e) and $C_{60}(OH)_{18}$ (f). The DOS of the fullerenols (black line) are compared with the one obtained for isolated C_{60} (grey line) and the zero of energy is set to the Fermi energy level (dashed lines).

different isomers, however it can indicate the stability tendency of highly hydroxylated fullerenes. Furthermore, considering the relative energy of these species, we obtain small energy differences for the isomers. In the case of the less symmetrical $C_{60}(OH)_8$ (figure 2(b)) the enthalpy of formation is only 1.5 eV higher than the corresponding enthalpy of the isomer displayed in figure 2(a). A similar relative stability is obtained for the two $C_{60}(OH)_{10}$ isomers shown in figures 2(c) and (d), for which the open-cage structure is less stable by 2.2 eV with respect to the structure given in figure 2(c).

Indeed, as can be seen in figure 5, the enthalpy of formation increases dramatically for higher hydroxylated fullerenes. Conversely, a large number of hydroxyl groups ($n > 36$) adsorbed on the fullerene surface can lead to unstable open-cage structures [31]. It is also interesting to notice that $-\Delta H_F/n$ can be interpreted as the adsorption enthalpy of the OH groups on the fullerene surface (see the inset in figure 5). Then, considering the adsorption of a single OH group we obtain a value of 1.54 eV, which indicates a mild chemisorption on the carbon cage, while for 24 OH groups well distributed on the C_{60} cage we obtain an adsorption enthalpy of 2.22 eV. The adsorption enthalpy increases for highly hydroxylated systems, i.e. for $n = 32$ and 36, for which we have estimated values of 2.8 and 3.4 eV, respectively, at the B3LYP/6–31G(d,p) level. From this point the molecular stability of the fullerenols with more numerous hydroxyl groups ($n = 40$–44) [31, 32] will largely depend on the particular location of these groups.

From the energetic analysis, we observe that highly polyhydroxylated fullerenes can give rise to structures with high chemical stability. Among these species, the optical absorption spectra of $C_{60}(OH)_{24–28}$ are of wide interest [25]. This is the case of $C_{60}(OH)_{24}$ that, additionally to its high formation energy, has a large HOMO–LUMO energy gap (as shown in the supplementary data, figure S4 (available at stacks.iop.org/Nano/19/365703)). These results seem to be in connection with the low cytotoxicity of a water-soluble $C_{60}(OH)_{24}$ isomer investigated by Sayes *et al* [17], when compared to colloidal solutions of C_{60} nanoparticles. In order

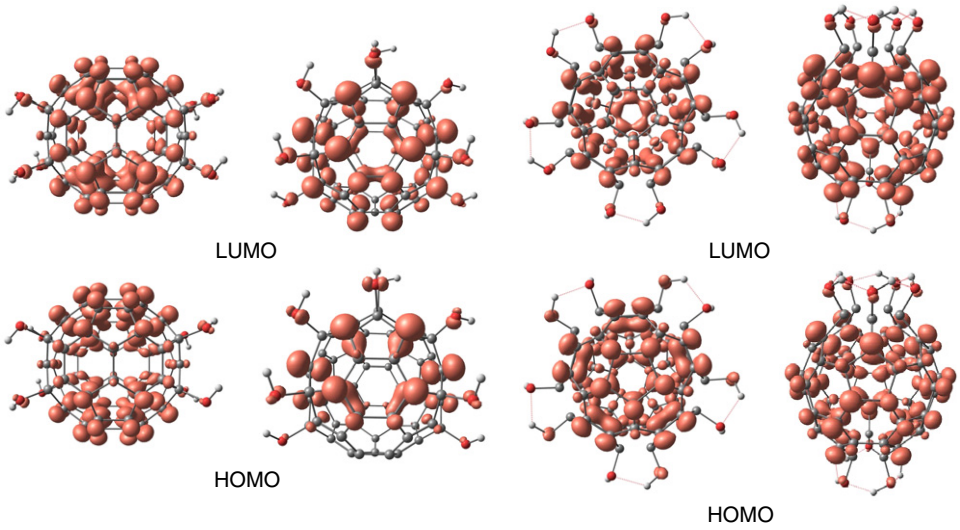

Figure 4. Partial charge densities of the HOMO–LUMO states of the $C_{60}(OH)_8$ (left) and $C_{60}(OH)_{10}$ (right) isomers displayed in figures 2(a)–(d). An isosurface of 0.008 au has been used in all these maps.

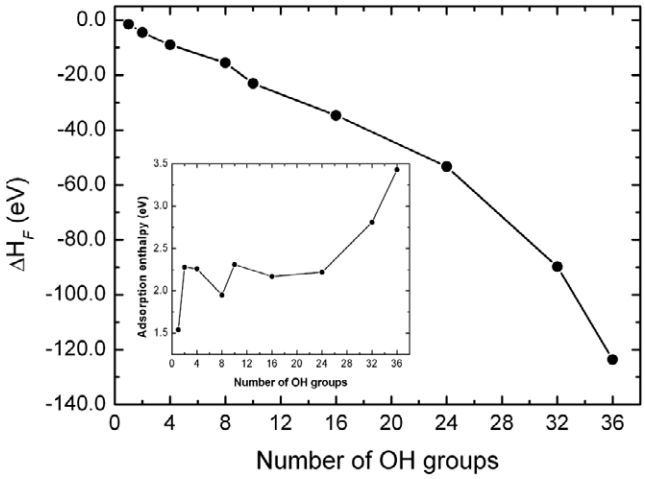

Figure 5. Calculated enthalpy of formation according to equation (1) for fullerenols with different degrees of hydroxylation, with the B3LYP/6–31G(d,p) level of theory. The isomers with 8 and 10 hydroxyl groups correspond to structures (a) and (c), respectively, presented in figure 2. The inset corresponds to $-\Delta H_F/n$ as a function of the number of hydroxyl groups.

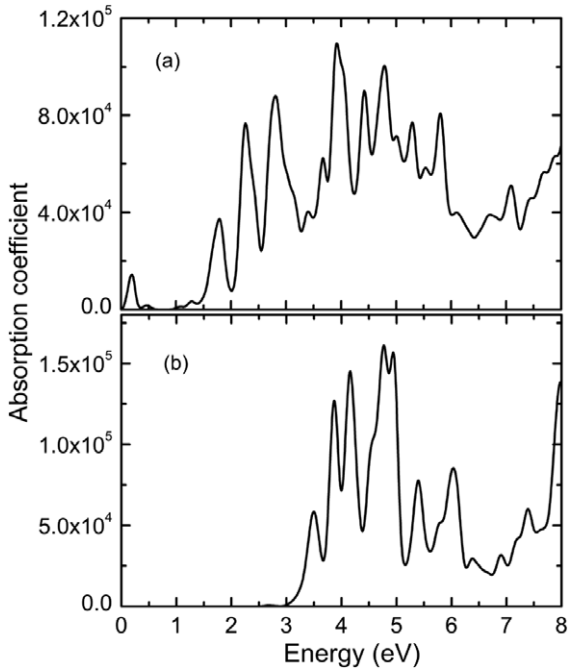

Figure 6. Calculated optical absorption spectra of $C_{60}(OH)_{18}$ (a) and $C_{60}(OH)_{24}$ (b) in the gas phase, with the BLYP/DZP level of theory. The calculations are performed from the position operator matrix elements between occupied and unoccupied single-electron eigenstates using first-order time-dependent perturbation theory (see more information in [36]). Gaussian functions with a width of 0.1 eV have been used to simulate a finite broadening of the spectra.

to better understand the 'inert' behavior of this fullerenol isomer, it is interesting to carefully analyze the calculated DOS of our proposed $C_{60}(OH)_{24}$ structure, shown in figure S4 (available at stacks.iop.org/Nano/19/365703). We can clearly notice a shift of the valence band to lower energies and the conduction band to higher energies, in comparison with the uncovered carbon cage. This effect is similar to the well-known quantum confinement effect observed in nanocrystals [41], which increases the bandgap as the system size decreases.

Also, from the present theoretical investigation we can address questions related to the optical properties of highly hydroxylated fullerenes. As already reported here, these structures can form hydrophilic species and are of great interest for diverse biological applications involving prominent photosensitizer properties. To investigate the optical spectra, we use the approach based on the dipolar transition matrix elements between different eigenfunctions of the self-consistent KS Hamiltonian, considering corrections due to the nonlocality of the pseudopotentials [36]. By using this approach, we analyze the optical properties of $C_{60}(OH)_{18}$ and $C_{60}(OH)_{24}$. The calculated optical absorption spectra in the gas phase of these fullerenol isomers are given in figure 6,

in the 0–8 eV energy range. As shown in figure 6(a), a small absorption in 0.19 eV is obtained in the $C_{60}(OH)_{18}$ spectrum. Nevertheless, the absorption properties in the 0–1 eV energy range are strongly dependent on the specific geometry (figure 2(e)) of the hydroxylated system. Indeed, the measurable absorptions seem to occur at 1.78 eV. This value is in agreement with experimental measurements of transient absorption [42] for $C_{60}(OH)_{18}$, which give a broad band around 650 nm, or equivalently at ca. 1.91 eV.

Now, considering the absorption spectrum of the $C_{60}(OH)_{24}$ structure given in figure S3 (available at stacks.iop.org/Nano/19/365703) we observe the first absorption peak at higher energies around 3.49 eV (figure 6(b)). Once again, this is in line with the total absence of optical transitions in the visible region of the spectra of fullerenol molecules containing between 24 and 28 OH groups [22]. Moreover, this is a good indicator of quantum confinement effects in this system and, consequently, of its high chemical stability in different environments. Actually, it has not been verified experimentally, from optical absorption measurements [25] of highly hydroxylated mixtures of $C_{60}(OH)_{24–26}$ and conjugated polymers, that there are appreciable changes in the absorption spectra of the fullerenols. This suggests that the polyhydroxylation of the fullerene cage may lead to a protective solvent layer, avoiding additional chemical attacks on the fullerenol surface or even strong interactions with the solvent. In contrast, the lower hydroxylated fullerenes seem to form more reactive species since their coverage is still below a complete monolayer.

4. Conclusions

We conclude this paper summarizing important features concerning the fullerenol molecules obtained by means of reliable DFT calculations. Our detailed electron structure analysis has shown that the degree of hydroxylation, along with the precise location of the OH groups, plays a crucial role in achieving tunable optical properties from fullerenols. For example, we have shown these molecules can exhibit bandgaps in a wide energy range by varying the disposition of the adsorbed hydroxyl groups, as in the case of the two isomers of $C_{60}(OH)_8$ and $C_{60}(OH)_{10}$ shown in figures 2(a)–(d). Consequently, the optical absorption properties of the fullerenols also depend on the external distribution of OH groups on the fullerene surface, as exhibited in the case of $C_{60}(OH)_{18}$ and $C_{60}(OH)_{24}$, given in figures 6(a) and (b), respectively.

Another important role of the hydroxyl group distribution, which appears for highly coated species (e.g. $n = 24$, 32 and 36), is related to their chemical reactivity. This was shown by the calculated adsorption enthalpy (figure 5), although a large number of hydroxyl groups ($n > 36$) can lead to unstable open-cage molecules. Also, quantum confinement effects may lead to negligible interactions between highly hydroxylated fullerenes and the surrounding solvent molecules. Such an effect has appeared in our proposed $C_{60}(OH)_{24}$ isomer. All these theoretical findings have been consistent with diverse experimental studies reported here, but more importantly, have yielded valuable information in the sense of identifying precise structures at the nanometer scale based on the electronic structure analysis.

Acknowledgments

This work has been partially supported by the Brazilian agencies FAPESB (Bahia), FAPESP (S. Paulo) and CNPq.

References

[1] Kroto H W, Heath J R, O'Brien S C, Curl R F and Smalley R E 1985 *Nature* **318** 162
[2] Rivelino R and Mota F B 2007 *Nano Lett.* **7** 1526
[3] Bedrov D, Smith G D, Davande H and Li L W 2008 *J. Phys. Chem.* B **112** 2078
[4] Ni J, Wu Q Y, Li Y G, Guo Z X, Tang G S, Sun D, Gao F and Cai J M 2008 *J. Nanoparticle Res.* **10** 643
[5] Nakamura E and Isobe H 2003 *Acc. Chem. Res.* **36** 807
[6] Kunsagi-Mate S, Vasapollo G, Szabo K, Bitter I, Mele G, Longo L and Kollar L 2008 *J. Incl. Phenom. Macrocycl. Chem.* **60** 71
[7] Nakae T, Matsuo Y and Nakamura E 2008 *Org. Lett.* **10** 621
[8] Chin K K, Chuang S C, Hernandez B, Campos L M, Selke M, Foote C S and Garcia-Garibay M A 2008 *Photochem. Photobiol. Sci.* **7** 49
[9] Mateo-Alonso A, Iliopoulos K, Couris S and Prato M 2008 *J. Am. Chem. Soc.* **130** 1534
[10] Qiao R, Roberts A P, Mount A S, Klaine S J and Ke P C 2007 *Nano Lett.* **7** 614
[11] Kolosnjaj J, Smarc H and Moussa F 2007 Toxicity studies of fullerenes and derivatives *Bio-Applications of Nanoparticles* (*Advances in Experimental Medicine and Biology* vol 620) ed W C W Chan (New York: Springer) p 168
[12] Injac R, Perse M, Boskovic M, Djordjevic-Milic V, Djordjevic A, Hvala A, Cerar A and Strukej B 2008 *Technol. Cancer Res.* T **7** 15
[13] Jacevic V, Djordjevic-Milic V, Dragojevic-Simic V, Radic N, Govedarica B, Dobric S, Srdjenovic B, Injac R, Djordjevic A and Vasovic V 2007 *Toxicol. Lett.* **172** S146
[14] Trajkovic S, Dobric S, Jacevic V, Dragojevic-Simic V, Milovanovic Z and Dordevic A 2007 *Colloids Surf.* B **58** 39
[15] Gelderman-Fuhrmann M P, Simakova O, Siddiqui S F, Vostal A C and Simak J 2006 *Blood* **108** 511A
[16] Badireddy A R, Hotze E M, Chellam S, Alvarez P and Wiesner M R 2007 *Environ. Sci. Technol.* **41** 6627
[17] Sayes C M *et al* 2004 *Nano Lett.* **4** 1881
[18] Isakovic A *et al* 2006 *Toxicol. Sci.* **91** 173
[19] Bogdanovic G, Kojic V, Dordevic A, Canadanovic-Brunet J, Vojinovic-Miloradov M and Baltic V V 2004 *Toxicol. In Vitro* **18** 629
[20] Milic V D, Djordjevic A, Dobric S, Injac R, Vuckovic D, Stankov K, Simic V D and Suvajdzic L 2006 *Recent Dev. Adv. Mater. Process.* **518** 529
[21] Kojic V, Jakimov D, Bogdanovic G and Dordevic A 2005 *Curr. Res. Adv. Mater. Process.* **494** 543
[22] Rincon M E, Guirado-Lopez R A, Rodriguez-Zavala J G and Arenas-Arrocena M C 2005 *Sol. Energy Mater. Sol. Cells* **87** 33
[23] Vileno B, Marcoux P R, Lekka M, Sienkiewicz A, Feher T and Forro L 2006 *Adv. Funct. Mater.* **16** 120
[24] Aikawa S, Yoshida Y, Nishiyama S, Noguchi H and Shoji A 2006 *Mol. Cryst. Liq. Cryst.* **445** 315
[25] Guirado-Lopez R A and Rincon M E 2006 *J. Chem. Phys.* **125** 154312
[26] Liu W J, Jeng U, Lin T L, Lai S H, Shih M C, Tsao C S, Wang L Y, Chiang L Y and Sung L P 2000 *Physica* B **283** 49

[27] Xia T, Kovochich M, Brant J, Hotze M, Sempf J, Oberley T, Sioutas C, Yeh J I, Wiesner M R and Nel A E 2006 *Nano Lett.* **6** 1794
[28] Pickering K D and Wiesner M R 2005 *Environ. Sci. Technol.* **39** 1359
[29] Rodriguez-Zavala J G and Guirado-Lopez R A 2004 *Phys. Rev.* B **69** 075411
[30] Rodriguez-Zavala J G and Guirado-Lopez R A 2006 *J. Phys. Chem.* A **110** 9459
[31] Xing G *et al* 2004 *J. Phys. Chem.* B **108** 11473
[32] Kokubo K, Matsubayashi K, Tategaki H, Takada H and Oshima T 2008 *ACS Nano* **2** 327
[33] Alves G C, Ladeira L O, Righi A, Krambrock K, Calado H D, Gil R and Pinheiro M V B 2006 *J. Braz. Chem. Soc.* **17** 1186
[34] Becke A D 1993 *J. Chem. Phys.* **98** 5648
[35] Lee C, Yang W and Parr R G 1988 *Phys. Rev.* B **37** 785
[36] Soler J M, Artacho E, Gale J D, Garcia A, Junquera J, Ordejon P and Sanchez-Portal D 2002 *J. Phys.: Condens. Matter* **14** 2745
[37] Junquera J, Paz O, Sanchez-Portal D and Artacho E 2001 *Phys. Rev.* B **64** 235111
[38] Becke A D 1993 *J. Chem. Phys.* **98** 5648
[39] Lee C, Yang W and Parr R G 1988 *Phys. Rev.* B **37** 785
[40] Frisch M J *et al* 2004 *Gaussian 03* revision D.01 (Wallingford, CT: Gaussian)
[41] Dalpian G M, Tiago M L, del Puerto M L and Chelikowsky J R 2006 *Nano Lett.* **6** 501
[42] Mohan H, Palit D K, Mittal J P, Chiang L Y, Asmus K D and Guldi D M 1998 *J. Chem. Soc. Faraday Trans.* **94** 359

Nanotechnology **19** (2008) 509801 (1pp) doi:10.1088/0957-4484/19/50/509801

Corrigendum

Effects of hydroxyl group distribution on the reactivity, stability and optical properties of fullerenols

E E Fileti, R Rivelino, F de Brito Mota and T Malaspina
2008 *Nanotechnology* **19** 365703

The values for the enthalpy of formation and adsorption enthalpy of $C_{60}(OH)_{32,36}$ presented in figure 5 are incorrect. We have calculated the complexation energies of these two compounds using the wrong values for the total energy of the pure C_{60}. The correct value of the C_{60} energy using B3LYP/6–31G(d,p) is −2286.174 031 au. Therefore, the complexation energies for $C_{60}(OH)_{32,36}$ should give −68.9 and −77.8 eV, respectively, and their adsorption enthalpies are in the same range of other moderately hydroxylated fullerenes. The authors regret these mistakes, which are entirely the fault of the authors. With these revisions, the correct graph is presented below.

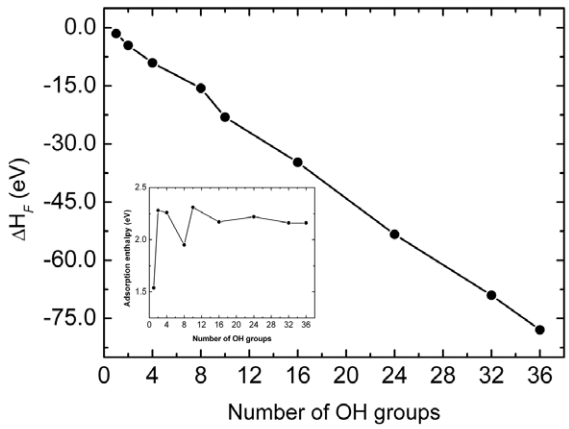

Figure 5. Calculated enthalpy of formation according to equation (1) for fullerenols with different degrees of hydroxylation, with the B3LYP/6–31G(d,p) level of theory. The isomers with 8 and 10 hydroxyl groups correspond to structures (a) and (c), respectively, presented in figure 2. The inset corresponds to $-\Delta H_F/n$ as a function of the number of hydroxyl groups.

